World Academy of Science, Engineering and Technology
International Journal of Aerospace and Mechanical Engineering
Vol:1, No:12, 2007

Modeling of Single-Particle Impact in Abrasive Water Jet Machining

S. Y. Ahmadi-Brooghani, H. Hassanzadeh, and P. Kahhal

Open Science Index, Aerospace and Mechanical Engineering Vol:1, No:12, 2007 publications.waset.org/12944.pdf

***Abstract*—**This work presents a study on the abrasive water jet (AWJ) machining. An explicit finite element analysis (FEA) of single abrasive particle impact on stainless steel 1.4304 (AISI 304) is conducted. The abrasive water jet machining is modeled by FEA software ABAQUS/CAE. Shapes of craters in FEM simulation results were used and compared with the previous experimental and FEM works by means of crater sphericity. The influence of impact angle and particle velocity was observed. Adaptive mesh domain is used to model the impact zone. Results are in good agreement with those obtained from the experimental and FEM simulation. The crater's depth is also obtained for different impact angle and abrasive particle velocities.

***Keywords*—**Abrasive water jet machining, Adaptive mesh control, Explicit finite elements analysis, Single-particle impact.

I. Introduction

INTEREST in advanced machining process (AMP) has been on the increasing demand due to vastly use of supper alloys, composites, and ceramics, which are difficult to or cannot be processed by traditional machining methods.

Some advantages of the AMP over the traditional machining processes are: better finishing of the area and lower tolerance, ability to create sub millimeter holes and etc.

AMP can be classified to three major fields: mechanical, thermo electrical and electrochemical processes. Abrasive Water Jet (AWJ) Machining is a mechanical advanced machining process. It is a machining process without much heat generation and the machined surface is virtually without any heat affected zone or residual stress. The AWJ machining is a non-contact, inertia-less cutting process that offers several advantages including narrow kerf width, negligible heat affected zone, and flexibility in material removing. Different types of abrasive is used in AWJ machining like garnet, olivine, aluminum oxide (Al_2O_3), silica-sand, glass bead, silicon carbide (Sic), zirconium, etc [1].

Manuscript received October 11, 2007.

S. Y. Ahmadi-Brooghani is with the Department of Mechanical Engineering, The University of Birjand, Birjand, Iran as Assistant Professor (phone: +985612227044; fax: +985612227795; e-mail: s.y.ahmadi@birjand.ac.ir).

H. Hassanzadeh is with the Department of Mechanical Engineering, The University of Birjand, Birjand, Iran as Assistant Professor (e-mail: Hassanzadeh42@yahoo.com).

P. Kahhal is with the Department of Mechanical Engineering, The University of Birjand, Birjand, Iran (e-mail: Parviz_pkl@yahoo.com).

In AWJ machining process, high velocity water containing abrasive particles is used to cut different materials ranging from soft to hard and ductile to brittle materials. Hard abrasive particles are accelerated in the cutting head by a high speed water jet to achieve the material cutting. The cutting head consists of an orifice, a mixing chamber, an abrasive inlet and a focusing tube. Water at pressures up to 400 MPa is pushed to flow through an orifice with a diameter between 0.1 and 0.3 mm where a high-speed water jet is generated. The velocity of water jet is proportional to the square root of water pressure and usually reaches to a value of about 1000 m/s [2]. The high speed water jet suck the abrasive material through the abrasive inlet. The abrasive material mixes with the water in mixing chamber, which is placed downstream the orifice. Abrasive particles are accelerated in focusing tube which its diameter is usually twice of the orifice diameter. During the suction of abrasive particles, air is entered through the abrasive inlet, and droplets start to generate around the jet and abrasive parts are fragmented during the acceleration. The resulting high speed jet of abrasive particles, water and air form the tool in the AWJ machining. Detail parts of cutting head in shown in Fig. 1.

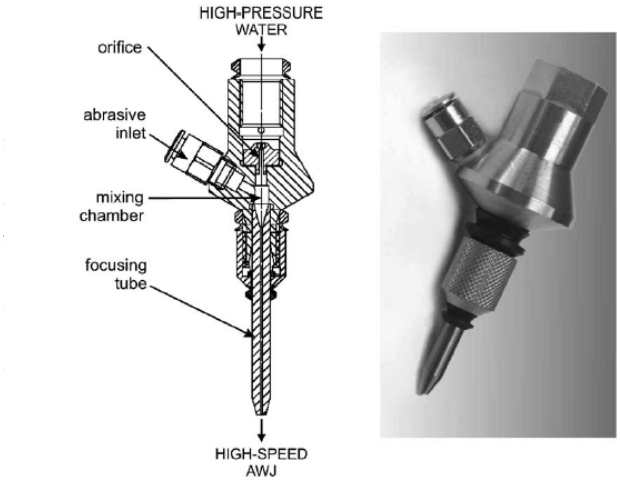

Fig. 1 AWJ cutting head [2]

The AWJ machining is a complex process, which is influenced by many parameters such as hydraulic, mixing, and abrasive parameters. Its capability to cut materials of different

Open Science Index, Aerospace and Mechanical Engineering Vol:1, No:12, 2007 publications.waset.org/12944.pdf

thickness depends on the choice of process parameters and the properties of materials being cut.

II. Previous Works

In order to understand the physics of the cutting process, many attempts have been made, by various approaches [3-9]. Orbanic and Junkar [3] used a cellular automata approach to simulate the AWJ machining process. They assumed a uniform energy distribution over the jet cross-section. The unit event approach has been used by Lebar and Junkar [4] to simulate the machining process. In this approach a uniform energy distribution is assumed and the amount of material which has been removed by a single abrasive particle at different impact angles has been found experimentally. A superposition of many unit events has been used to predict the generated surface.

Henning and Westkamper [5] used a phenomenological approach to simulate the generated surface. They assumed a Gaussian distribution of the jet energy and the generated surface is simulated by taking into account different wear mechanisms as a function of the impact angle and the energy concentration at different points of the jet cross-section. Vikram and Ramesh Babu [6] modeled 3D topography of the surface cut by AWJ. They used the ballistic theory to predict the trajectory of the jet in the workpiece material and Bitter's theory of erosion to predict the material removal. Momber *et al.* [7] has reported several models and approach for simulating the AWJ machining. All the models simulate the process of the material removing by AWJ. The consequences of these models are the generated surface on the workpiece.

The Finite Element Method (FEM) is a powerful tool to simulate the material removing process. Many researchers have been conducted to evaluate the effect of different process parameters. Guo *et al.* [8] made an implicit FEM simulation of the AWJ drilling process, which was validated by an optical technique. They analyzed the stress field in the specimen due to a static load of the jet. The validation was executed by a Moiré interferometery technique. Hassan and Kosmol [9] used an implicit FEA approach to simulate the erosion of a single abrasive particle.

Some researchers have neglected the dynamics effects in the AWJ process modeling [5 , 9]. They ignored the effects of velocity and acceleration also in some cases they considered the elastic behavior of material which means plastic deformation has been neglected. These assumptions are not appropriate for real impact in AWJ machining. In the impact problems usually plastic deformation occur near or in the impact zone.

Molinari and Ortiz [10] have modeled a single-particle impact using FEA. They simulated impacts of a solid particle on a metallic target at 3 different particles velocities and impact angles. The size of particle which has been used in their analysis is 100 times bigger than the real particles and the size of particle which has been used in this work.

Junkar *et al.* [2] Simulated single-particle impact in AWJ and experimentally validated their simulation. They analyzed the effect of a single abrasive particle impact on the workpiece material using an explicit FEA. The simulations results were compared and validated with the experimental results by means of crater's sphericity. A piecewise linear plasticity material model has been used for their simulation. The impact of single particle has been simulated in 3 different velocities and 3 different impact angles (totally 9 simulations). In experimental verification for each of the nine sets of the process parameters, 200 craters were examined. Pictures of craters were taken and from each set they picked a crater of average size and shape. They considered dynamic properties such as velocity and gravity, and modeled elastic–plastic behavior of workpiece material. ANSYS/LS-DYNA is used for their simulation. They computed the velocity of abrasive particle as a function of water pressure then compared the results with each other. The trend of their FEM results is in good agreement with the experimental results. One of the reasons which may affect the accuracy of the results comparing with the experimental results is the assumption of piecewise linear plastic deformation and ignoring the effect of strain rate. Assuming linear plastic deformation by Junkar *et al.* [2] may affect the accuracy of the modeling. The plastic behavior of the material is non-linear and more accurate model, like Johnson-Cook which is nonlinear model and rate dependant, can improve the results.

One of the aims of this work is to improve the Junkar *et al.* [2] model by FEM in two direction, (a) using the Johnson-Cook model which provide more accurate material behavior, (b) the use of adaptive mesh in the impact zone. Also in this work the effect of the impact angle and particle velocity on the depth of crater has been studied.

III. FEM Simulation

FEM was successfully applied in numerous fields of manufacturing. It proves itself as a powerful tool for design, evaluation and optimization of new products and processes. FEM drastically reduces product development time and costs.

The impact of high speed abrasive particle with workpiece is a complex problem which many parameters are involved. For example since the impact velocity is high, the strain rate effect cannot be ignored. For these reasons the Johnson-Cook material model has been used for the workpiece. Johnson-Cook plasticity model is a particular type of Mises plasticity model with analytical forms of the hardening law and rate dependence. It is suitable for high-strain-rate deformation of many materials, including most metals and typically used in adiabatic transient dynamic simulations. Johnson-Cook hardening is a particular type of isotropic hardening where the static yield stress, σ^0, is assumed to be of the form:

$$\sigma^0 = \left[A + B\left(\bar{\varepsilon}^{pl}\right)^n \right]\left(1-\hat{\theta}^m\right) \quad (1)$$

where $\bar{\varepsilon}^{pl}$ is the equivalent plastic strain and A, B, n and m are material parameters measured at or below the transition

Open Science Index, Aerospace and Mechanical Engineering Vol:1, No:12, 2007 publications.waset.org/12944.pdf

temperature, θ_{tran} defined as the one at or below which there is no temperature dependence on the expression of the yield stress. The dimensionless temperature $\hat{\theta}$ is defined as:

$$\hat{\theta}=\begin{cases} 0 & \text{for} \quad \theta<\theta_{tran} \\ \dfrac{(\theta-\theta_{tran})}{(\theta_{melt}-\theta_{tran})} & \text{for} \quad \theta_{tran}\le\theta\le\theta_{melt} \\ 1 & \text{for} \quad \theta>\theta_{melt} \end{cases} \tag{2}$$

where θ_{melt} is the melting temperature.

Johnson-Cook strain rate dependence assumes that:

$$\bar{\sigma}=\sigma^0\left(\bar{\varepsilon}^{pl},\theta\right)R\left(\dot{\bar{\varepsilon}}^{pl}\right) \tag{3}$$

and

$$\dot{\bar{\varepsilon}}^{pl}=\dot{\varepsilon}_0\exp\left[\frac{1}{C}(R-1)\right] \quad for\ \bar{\sigma}\ge\sigma^0 \tag{4}$$

where σ^0 is the yield stress at nonzero strain rate, $\dot{\bar{\varepsilon}}^{pl}$ is the equivalent plastic strain rate, $\dot{\varepsilon}_0$ and C are material parameters measured at or below the transition temperature, $\sigma^0(\bar{\varepsilon}^{pl},\theta)$ is the static yield stress and $R(\dot{\bar{\varepsilon}}^{pl})$ is the ratio of the yield stress at nonzero strain rate to the static yield stress (so that $R(\dot{\bar{\varepsilon}})=1.0$). The yield stress is, therefore, expressed as [11]:

$$\bar{\sigma}=\left[A+B(\bar{\varepsilon}^{pl})^n\right]\left[1+C\ln\left(\frac{\dot{\bar{\varepsilon}}^{pl}}{\dot{\varepsilon}_0}\right)\right]\left(1-\hat{\theta}^m\right) \tag{5}$$

Material properties and Johnson–Cook parameters of the stainless steel 1.4304 (AISI 304) which we used for workpiece material are given in Table I [12].

Adaptive mesh domain has been used in this simulation by ABAQUS/CAE. Adaptive mesh domain usually used in metal forming simulations to predict the behavior of workpiece more accurately. Adaptive mesh domain defines the parts of a finite element model where mesh movement is independent of material deformation. It has boundary regions where loads, boundary conditions, and surfaces can be defined. Adaptive mesh domain smoothes impact area mesh and is very suitable for this simulation because of the complexity of impact.

The contact between abrasive particle and workpiece modeled using STS (surface to surface) type. The workpiece material was modeled with 3D solid (Hex) elements. The size of element was controlled, so that the mesh size is finer at the impact region and gradually increases the mesh size as the distance from the impact region increase. The abrasive particle was modeled using 3D solid (Hex) elements. The geometry and material properties of the abrasive particles are shown in Table II. Since the abrasive particles are fragmented during the acceleration and in the mixing chamber the size of the particles are reduced. As mentioned by Junklar *et al.* [2] the initial abrasive particle diameter is 190 μm but in the simulation and the present work the diameter of the particle is assumed to be 100 μm. A single abrasive particle impact was simulated using an explicit FEA at 3 different impact velocities and 5 different impact angles (totally 15 different states) as listed in Table III.

TABLE I
MATERIAL PROPERTIES AND JOHNSON-COOK PARAMETERS FOR STAINLESS STEEL 1.4304 (AISI 304)

Density (Kg/m^3)	7900
Young modulus (GPa)	200
Poisson's ratio	0.3
Melting temperature (K)	1673
Transition temperature (K)	1000
Specific heat (J/Kg K)	440
A (MPa)	310
B (MPa)	1000
n	0.65
c	0.07
$\dot{\varepsilon}_0$ (s^{-1})	1.00
m	1.00

TABLE II
GEOMETRY AND MATERIAL PROPERTIES OF ABRASIVE PARTICLES

Particles shape	Spherical
$d_{A,FEA}$, particles diameter (μm)	100
$\rho_{A,FEA}$, abrasive density (Kg/m^3)	4000
E_A, elasticity module (MPa)	2.48×10^5
ν_A, Poisson's coefficient	0.27

TABLE III
PROCESS PARAMETERS SETUP IN FEM SIMULATIONS

v_A, particle velocity at the impact (m/s)	180
	200
	220
α_I, impact angle (Deg)	90
	75
	60
	45
	30

IV. RESULTS

The finite element analysis has been performed using ABAQUS/CAE on a Pentium IV computer. The material properties of workpiece have been modeled using Johnson-Cook model as described in Table I. The adaptive mesh domain was used to model the impact region and material deformation.

Open Science Index, Aerospace and Mechanical Engineering Vol:1, No:12, 2007 publications.waset.org/12944.pdf

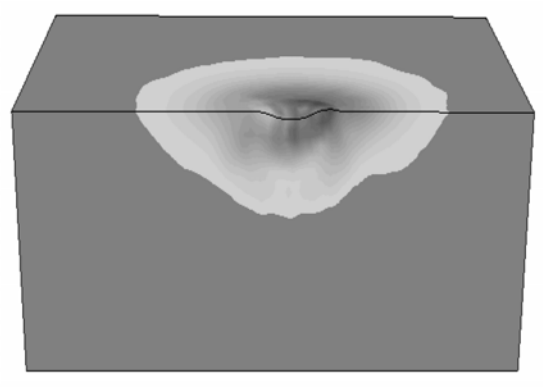

α =30°, v =180 m/s

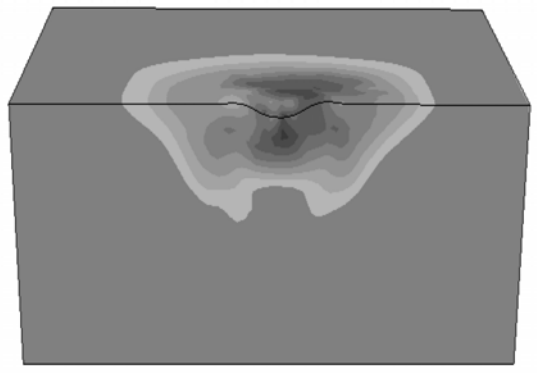

α =60°, v =180 m/s

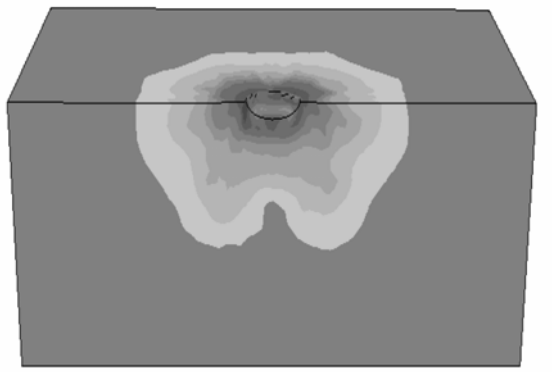

α =90°, v =180 m/s

Fig. 2 Resulting impact region

Based on the mentioned condition and Table III, five different impact angles and three different velocities of particle have been considered. Fig. 2 shows the impact region after the abrasive particle has been impingement for the three impact angles and the velocity of 180 m/s. It shows the created defect (crater) dimension (the area and the depth). As one can see the particle has moved the material in the velocity direction. Also it is noticeable that the deformation is local and the material away from the impact region is not affected.

The results which have been obtained using these analyses were compared with the Junkar *et al.* [2] work (simulation and experiments). The sphericity of craters has been computed for each state of simulation. Sphericity is a criterion of deformed material after the impact and defined as the ratio of the minor crater dimension d_1 over the major crater dimension d_2 as illustrated in Fig. 3.

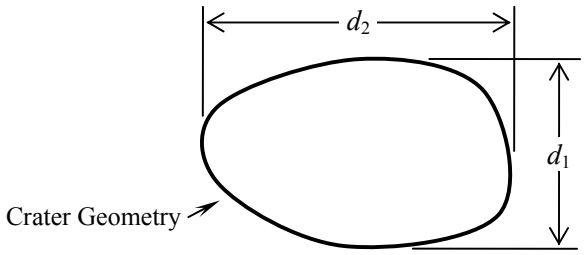

Fig. 3 Crater's sphericity

In order to verify the results of the present study the results have been compared with those reported by Junkar *et al.* [2]. They have reported their experimental and finite element modeling results in three impact angles (30°, 60° and 90°) and three different particle velocities (180m/s, 200m/s and 220m/s) and the associated pressure in experimental work. The analysis in present work is in five impact angles (30°, 45°, 60°, 75° and 90°) and three particle velocities (180m/s, 200m/s and 220m/s). The workpiece material is the same in both works. Fig. 4 shows the results of the present study for the sphericity of craters. It shows a good agreement with the experimental work comparing to the Junkar *et al* [2] FEM modeling. It seems that the material behavior model using Johnson-Cook material model shows more accurate results. The use of finer mesh in the impact area is necessary due to the large deformation in the impact area but there is no need to have finer mesh in the area away from the impact zone.

The sphericity for the impact angle of 90° is the same for the present and the Junkar *et al.* [2] FEM work since the particle is assumed to be spherical. In the experimental work of Junkar *et al.* [2] the real shape of the particles are not sphere, which means that the crater shape will not be a circle, so the sphericity will be less than 1.

For the impact angle less than 90°, the sphericity will decrease to less than 1 since the horizontal component of the velocity (momentum) will move the material in the velocity direction. In the impact angle of 60°, the present results are approaching to the experimental results since the effect of the particles shape decrease and the deformation due to the momentum of particle in horizontal direction is more effective.

The diversity of the present work from the experimental work of Junkar et al. [2] is more at the impact angle of 30°; however it is better than FEM model of Junkar et al. [2]. It seems that in the impact angle of 30° the horizontal component of the velocity (momentum) is more effective than the vertical component; therefore the effect of surface roughness and hardness at the surface is more effective so that the result is not as accurate as in the impact angle of 60°.

The relative difference between measured sphericity in Junkar et al. [2] experiments and our simulated sphericity was calculated according to:

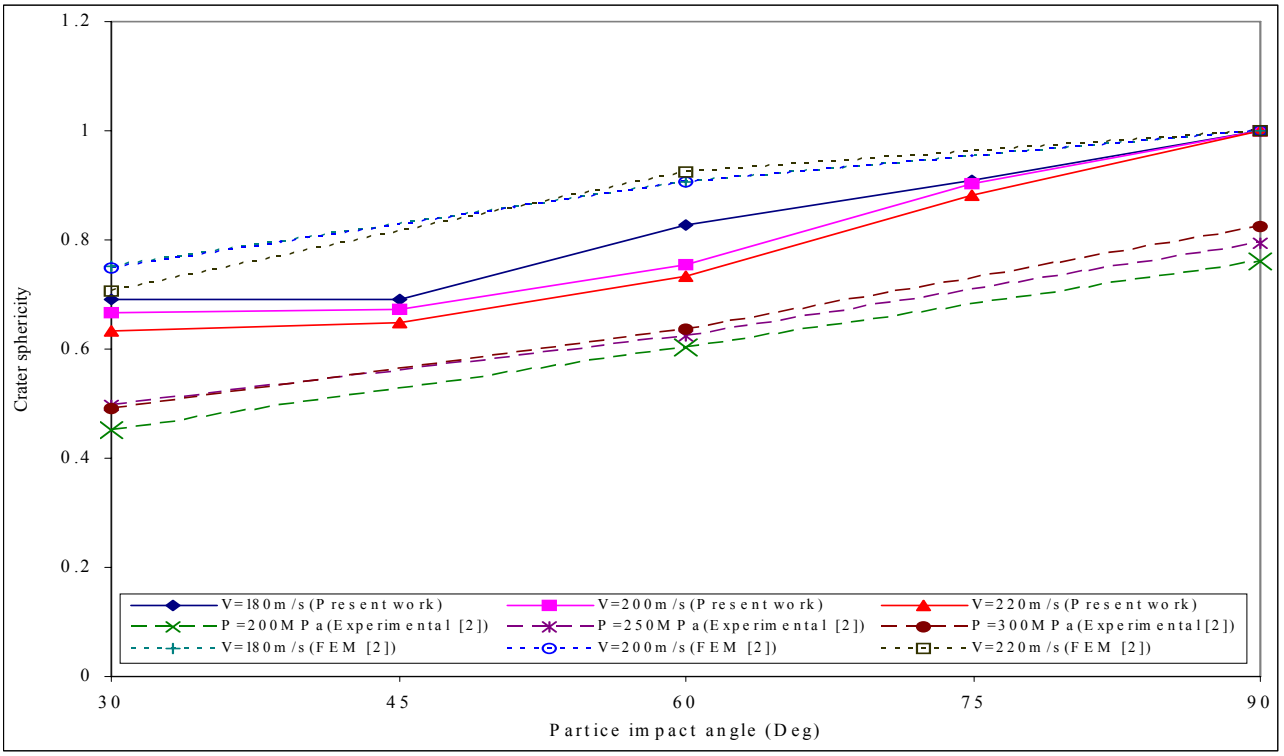

Fig. 4 Comparing of the crater's sphericity for different analysis

$$\Delta_S = \frac{S_{C,FEA} - S_{C,Exp}}{S_{C,FEA}} 100\%. \quad (6)$$

Relative differences between FEA simulations and experimental measurements of Junkar *et al.* [2] and the relative differences between present simulation and experimental measurements of Junkar *et al.* [2] are presented in Table IV. The numerical values of sphericity are showed in the Table IV.

The effect of the abrasive particle impact is the crater which has been created during the impact. The crater depth is another criterion which is necessary to be considered. In the present work the crater's depth was calculated for different velocities and impact angle of the particles. Fig. 5 shows the depth of the craters vs. velocity and impact angles. As one can see the depth is increased as the velocity and impact angle is increased. It is obvious since the particle has more energy and momentum and therefore the stress and the deformation on the work increase.

V. Conclusion

An analysis of a single abrasive particle impact on the workpiece surface in AWJ machining has been done. The explicit FEM simulations of single-particle impacts at different angles and velocities have been conducted and the results have been compared with latest previous work [2]. The results show a good agreement with the previous experimental and FEM work [2]. The depths of the craters are also calculated and have been presented.

A basic model of a single abrasive particle impact is defined. Two process parameters, particle velocity and the impact angle, have been studied.

From the present work, the following conclusions can be observed:

- An explicit FEM simulation is suitable for better understanding of the AWJ machining process and influences of process parameters on it.
- When impact angle increases, the crater's sphericity increase approaching to 1.
- When velocity of particle increases, the crater's sphericity decreases.
- When the impact angle is set to 90°, the crater shape depends on abrasive particles shape.
- Cutting depth has increases when particle velocity or impact angle increases.
- As mentioned by Junkar *et al.* [2], the process at small angles and smaller velocities (water pressures), is more complex, because abrasive particle shape, workpiece surface integrity, etc, have a stronger effect on the shape of the craters.
- Results from explicit FEM simulation are in good agreement with previous experimental work.

For further FEM simulations, more attention can be dedicated to the influence of abrasive particles shape and size, the fragmentation of abrasive particles and their acceleration, friction conditions at the impact interface and characteristics of the workpiece surface.

Open Science Index, Aerospace and Mechanical Engineering Vol:1, No:12, 2007 publications.waset.org/12944.pdf

TABLE IV
COMPARISON PRESENT SIMULATION WITH JUNKAR ET AL. [2] BY MEANS OF RELATIVE DIFFERENCE

Impact angle α_I (Deg)	30	45	60	75	90
1. Measured sphericity at P_W= 200 MPa by Junkar *et al.* [2]	0.4525	-	0.6034	-	0.7595
2. Simulated sphericity at v_A = 180 m/s by Junkar *et al.* [2]	0.7530	-	0.9058	-	1.0000
3. Simulated sphericity at v_A = 180 m/s in present work	0.6924	0.6903	0.8271	0.9089	1.0000
4. Relative difference, Δ_S (%) between 1 & 2 (Junkar *et al.* [2] Comparing)	39.9	-	**33.4**	-	**24.0**
5. Relative difference, Δ_S (%) between 1 & 3 (this work Comparing)	34.65	-	**27.04**	-	**24.0**
1.Measured sphericity at P_W= 250 MPa by Junkar *et al.* [2]	0.4984	-	0.6239	-	0.7933
2.Simulated sphericity at v_A = 200 m/s by Junkar *et al.* [2]	0.7479	-	0.9058	-	1.0000
3. Simulated sphericity at v_A = 200 m/s in present work	0.6667	0.6736	0.7556	0.9018	1.0000
4. Relative difference, Δ_S (%) between 1 & 2 (Junkar *et al.* [2] Comparing)	**33.4**	-	**31.1**	-	**20.7**
5. Relative difference, Δ_S (%) between 1 & 3 (this work Comparing)	**25.24**	-	**17.42**	-	**20.7**
1.Measured sphericity at P_W= 300 MPa by Junkar *et al.* [2]	0.4922	-	0.6375	-	0.8254
2.Simulated sphericity at v_A = 220 m/s by Junkar *et al*. [2]	0.7051	-	0.9242	-	1.0000
3. Simulated sphericity at v_A = 220 m/s in present work	0.6342	0.6497	0.7333	0.8818	1.0000
4. Relative difference, Δ_S (%) between 1 & 2 (Junkar *et al.* [2] Comparing)	**30.2**	-	**31.0**	-	**17.5**
5. Relative difference, Δ_S (%) between 1 & 3 (this work Comparing)	**22.39**	-	**13.06**	-	**17.5**

It is advisable to consider other shapes like diamond to be used for particles.

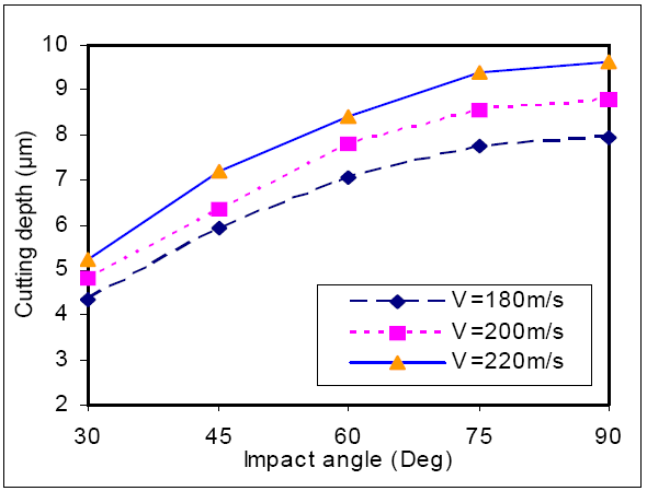

Fig. 5 Cutting depth

REFERENCES

[1] A. A. Khan, M. M. Haque, "Performance of different abrasive materials during abrasive water jet machining of glass", Journal of materials processing technology 191 (2007) 404-407.

[2] M. Junkar, B. Jurisevic, M. Fajdiga, M. Grah, "Finite element analysis of single-particle impact in abrasive water jet machining", International Journal of Impact Engineering 32 (2006) 1095–1112.

[3] Orbanic H, Junkar M. "Cellular automata in mechanical engineering". In: Junkar M, Levy PR, editors. Proceedings of the sixth international conference on management of innovative technologies. Piran, Slovenia: LAT, TAVO; 2003. p. 139–47.

[4] Lebar A, Junkar M. "Simulation of abrasive waterjet machining based on unit event features". Proc Inst Mech Eng BJ Eng Manuf 2003; 217(B5):699–703.

[5] Henning A, Westkamper E. "Modeling of wear mechanisms at the abrasive waterjet cutting front". In: Summers DA, editor. Proceedings of the 2003 WJTA American waterjet conference. Houston, TX, USA: WJTA; 2003. Paper 3-A.

[6] Vikram G, Ramesh Babu N. "Modelling and analysis of abrasive water jet cut surface topography". Int J Mach Tools Manuf 2002; 42:1345–54.

[7] Momber AW, Kovacevic R. "Principles of abrasive water jet machining". Berlin: Springer; 1998.

[8] Guo Z, Ramulu M, Jenkins MG. "Analysis of the waterjet contact/impact on target material". Opt Lasers Eng 2000; 33:121–39.

[9] Hassan AI, Kosmol J. "Finite element modeling of abrasive water-jet machining (AWJM)". In: Ciccu R, editor. 15th international conference on jetting technology. Ronneby (Sweden): BHR Group Limited; 2000. p. 321–33.

[10] Molinari JF, Ortiz M. "A study of solid-particle erosion of metallic targets". Int J Impact Eng 2002; 27:347–58.

[11] Abaqus Version 6.4 Documentation.

[12] S. Lee, F. Barthelat , J.W. Hutchinson , H.D. Espinosa , "Dynamic failure of metallic pyramidal truss core materials – Experiments and modeling". International Journal of Plasticity 22 (2006) 2118–2145.

Open Science Index, Aerospace and Mechanical Engineering Vol:1, No:12, 2007 publications.waset.org/12944.pdf